Cell Stem Cell
Article

Neural Stem Cells Confer Unique Pinwheel Architecture to the Ventricular Surface in Neurogenic Regions of the Adult Brain

Zaman Mirzadeh,[1,2] Florian T. Merkle,[1,2] Mario Soriano-Navarro,[3] Jose Manuel Garcia-Verdugo,[3] and Arturo Alvarez-Buylla[1,2,*]
[1]Department of Neurosurgery
[2]Developmental and Stem Cell Biology Program
University of California, San Francisco, San Francisco, CA 94143, USA
[3]Laboratorio de Morfología Celular, Unidad Mixta CIPF-UVEG, CIBERNED, Valencia 46012, Spain
*Correspondence: abuylla@stemcell.ucsf.edu
DOI 10.1016/j.stem.2008.07.004

SUMMARY

Neural stem cells (NSCs, B1 cells) are retained in the walls of the adult lateral ventricles but, unlike embryonic NSCs, are displaced from the ventricular zone (VZ) into the subventricular zone (SVZ) by ependymal cells. Apical and basal compartments, which in embryonic NSCs play essential roles in self-renewal and differentiation, are not evident in adult NSCs. Here we show that SVZ B1 cells in adult mice extend a minute apical ending to directly contact the ventricle and a long basal process ending on blood vessels. A closer look at the ventricular surface reveals a striking pinwheel organization specific to regions of adult neurogenesis. The pinwheel's core contains the apical endings of B1 cells and in its periphery two types of ependymal cells: multiciliated (E1) and a type (E2) characterized by only two cilia and extraordinarily complex basal bodies. These results reveal that adult NSCs retain fundamental epithelial properties, including apical and basal compartmentalization, significantly reshaping our understanding of this adult neurogenic niche.

INTRODUCTION

New neurons and glial cells continue to be born in restricted germinal regions in the adult mammalian brain (Alvarez-Buylla and Lim, 2004; Zhao et al., 2008). The largest germinal region of the adult brain is found on the walls of the lateral ventricles. In this region, primary neural progenitors reside in the subventricular zone (SVZ), displaced from the ventricles by ependymal cells. In contrast, primary neural progenitors in the developing brain reside in the ventricular zone (VZ), a pseudostratified epithelium in direct contact with the embryonic brain ventricles. Contact with the ventricle through an apical process is critical for maintaining germinal activity of the primary progenitors in the developing brain (Bittman et al., 1997; Nadarajah et al., 1997; Kosodo et al., 2004; Weissman et al., 2004). It is therefore intriguing that the primary progenitors in the adult brain are displaced from the ventricle.

In the embryonic VZ, the primary neural progenitors are radial glia (Noctor et al., 2007b). These elongated stem cells maintain contact with both the pial surface and the ventricular surface. Shortly after birth, however, radial glia transform into parenchymal astrocytes (Voigt, 1989) and ependymal cells (Spassky et al., 2005), and little remains of their unique morphology and behavior as the VZ is replaced by the ependymal epithelium.

Adult neural stem cells (NSCs) in the SVZ generate large numbers of olfactory bulb interneurons and some oligodendrocytes in corpus callosum, fimbria, and striatum (Jackson and Alvarez-Buylla, 2008). These primary progenitors have been identified as a subpopulation of astrocytes called type B1 cells (Doetsch et al., 1999a), which are derived from radial glia (Merkle et al., 2004). Interestingly, it has been shown that a small subpopulation of SVZ B1 cells have an apical membrane that contacts the ventricle and that the number of these contacts appears to be increased when SVZ proliferation is stimulated (Doetsch et al., 1999b). For radial glia in the embryo, this apical membrane is a specialized structure enriched in prominin-1 (CD133) (Weigmann et al., 1997), par-3 (Manabe et al., 2002), and numb (Rasin et al., 2007). It is the site where the primary cilium, basal body, and daughter centriole are located during interphase (Cohen et al., 1988), where the nucleus migrates for mitosis (Committee, 1970), and where the midbody is found at the end of cytokinesis (Dubreuil et al., 2007). Recent evidence suggests that the apical membrane may determine the symmetry of radial glial cell division (Kosodo et al., 2004). The apical membrane of the ventricle-contacting B cells is therefore a potentially important link between adult neurogenesis from the SVZ and developmental neurogenesis from the VZ, and may yield many insights into adult NSC function and niche organization.

We developed a new technique to study the apical and basal specializations and organization of different cell types that touch the ventricle in the adult brain. We find that most, if not all, B1 cells comprise a modified VZ in the adult brain with apical contacts and a unique pinwheel architecture. We have also characterized a type of ependymal cell with two cilia and a previously undescribed basal body. This significantly reshapes our understanding of the architecture of this adult neurogenic niche. The work suggests that a neurogenic VZ persists in the adult mammalian brain.

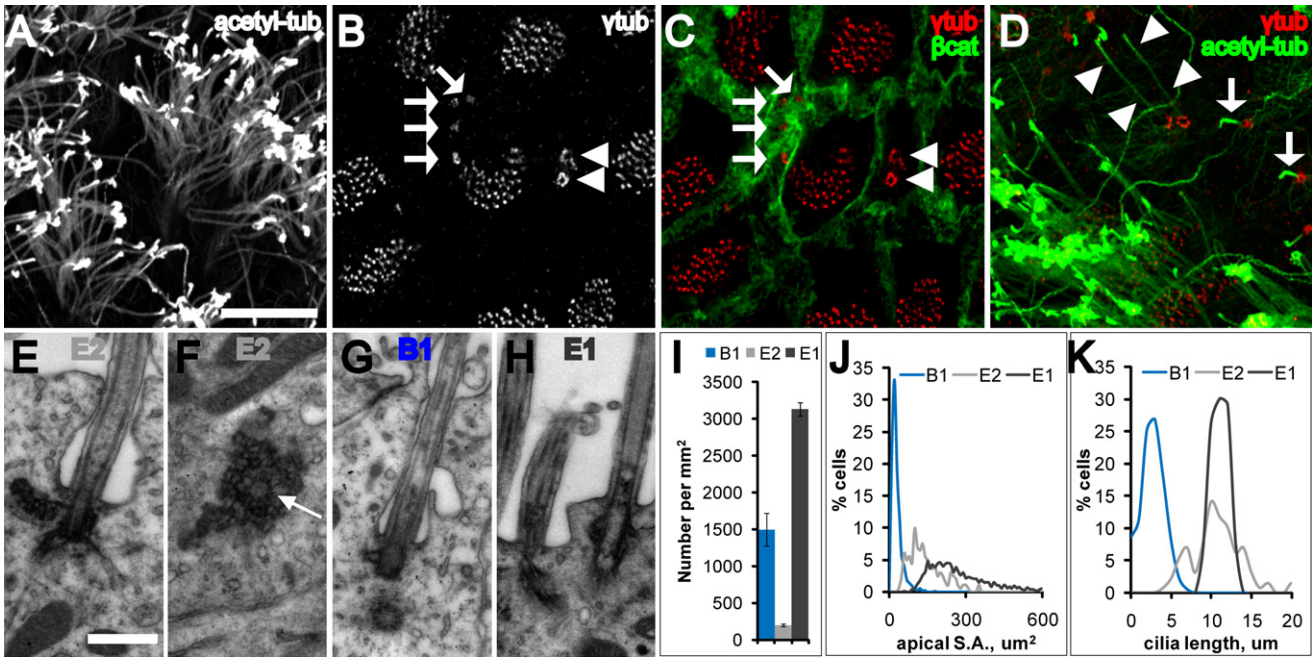

Figure 1. Three Cell Types Contact the LV

(A–D) Confocal images taken at the surface of whole mounts of the lateral wall of the LV. (A) Acetylated tubulin staining reveals many long cilia of ependymal cells. Scale bar, 10 μm (A–D). (B and C) γ-tubulin staining (B) together with β-catenin staining (C) reveals three cell types: E1 (clusters of small basal bodies), B1 (arrows indicate single basal body), and E2 (arrowheads indicate two basal bodies). (D) Three cell types are also distinguished by their cilia. B1 cells have a single short cilium (arrows), and E2 cells have two long cilia (arrowheads).

(E and F) Electron micrographs from two serially reconstructed E2 cells. The central barrel of the basal body is cut transversely in (E) and in crosssection in (F) (arrow). Scale bar, 0.5 μm (E–H).

(G) Electron micrograph of the primary cilium, basal body, and centriole of a B1 cell. Note the simpler B1 basal body compared with the large, lobular E2 basal body (F). Both B1 and E2 (E) cilia were invaginated in the apical membrane.

(H) Electron micrograph of E1 cilia, which were not invaginated.

(I) Density of B1, E1, and E2 cells on the lateral wall of the LV. Error bars show SEM.

(J) Histogram of apical surface area of B1, E1, and E2 cells. Data from 771 B1 cells, 1716 E1 cells, and 201 E2 cells from n = 4 mice.

(K) Histogram of cilia length of B1, E1, and E2 cells. Data from 361 B1 primary cilia, 55 ependymal cilia, and 106 E2 cilia from n = 3 mice.

RESULTS

Three Cell Types Contact the Lateral Ventricle

Whole mounts provide an en face view of the ventricular surface (see Figure S1 available online) (Doetsch and Alvarez-Buylla, 1996), which we hypothesized would facilitate the identification of ventricle-contacting cells. For this study, whole mounts were dissected from mice 60–120 days old. The ventricular surface was largely covered by tufts of ependymal cilia obstructing a clear view of cells that may lie behind (Figure 1A). To obtain an unobstructed view of the ventricular surface, we used γ-tubulin antibodies to label basal bodies and β-catenin antibodies to delineate the cell membrane (Figures 1B and 1C). This revealed three distinct cellular profiles in contact with the lateral ventricle (LV): (1) cells with a large apical surface and multiple (32–73, mean 49) basal bodies, with γ-tubulin distributed as small, individual points (diameter, 0.54 μm) at each basal body; (2) cells with a small apical surface and a single basal body, with γ-tubulin distributed in a donut configuration (diameter, 0.94 μm) presumably around the basal body in the pericentriolar material tube (Ou et al., 2004); and (3) cells with an intermediate-sized apical surface and two large, complex basal bodies, with more intense γ-tubulin expression distributed in small, individual points as in (1), but arranged in large donut or horseshoe formations (diameter, 1.35 μm). Costaining for γ-tubulin and acetylated tubulin revealed that these three cell types could also be distinguished by their cilia (Figure 1D): (1) cells with multiple basal bodies had multiple long cilia, corresponding to ependymal cells; (2) cells with a single basal body had a single, short primary cilium, corresponding to B1 cells; and (3) cells with complex basal bodies were often biciliated, with long cilia comparable to those of ependymal cells. We will refer to these biciliated cells as E2 cells and to multiciliated ependymal cells as E1 cells.

To our knowledge, E2 cells have not been described before (see references in the Discussion). To characterize the ultrastructure of E2 cells, we reconstructed several of them by transmission electron microscopy (TEM) (Figures 1E and 1F and Figures S2 and S3). E2 cells had two basal bodies, deep interdigitations of the cell membrane with long lateral extensions, light cytoplasm, and spherical nuclei with no invaginations and dispersed chromatin. Mitochondria were abundant, but unlike E1 cells where mitochondria localize near the basal bodies, in E2 cells they were concentrated around the nucleus. Small dictyosomes similar to those observed in E1 cells were also present. The main

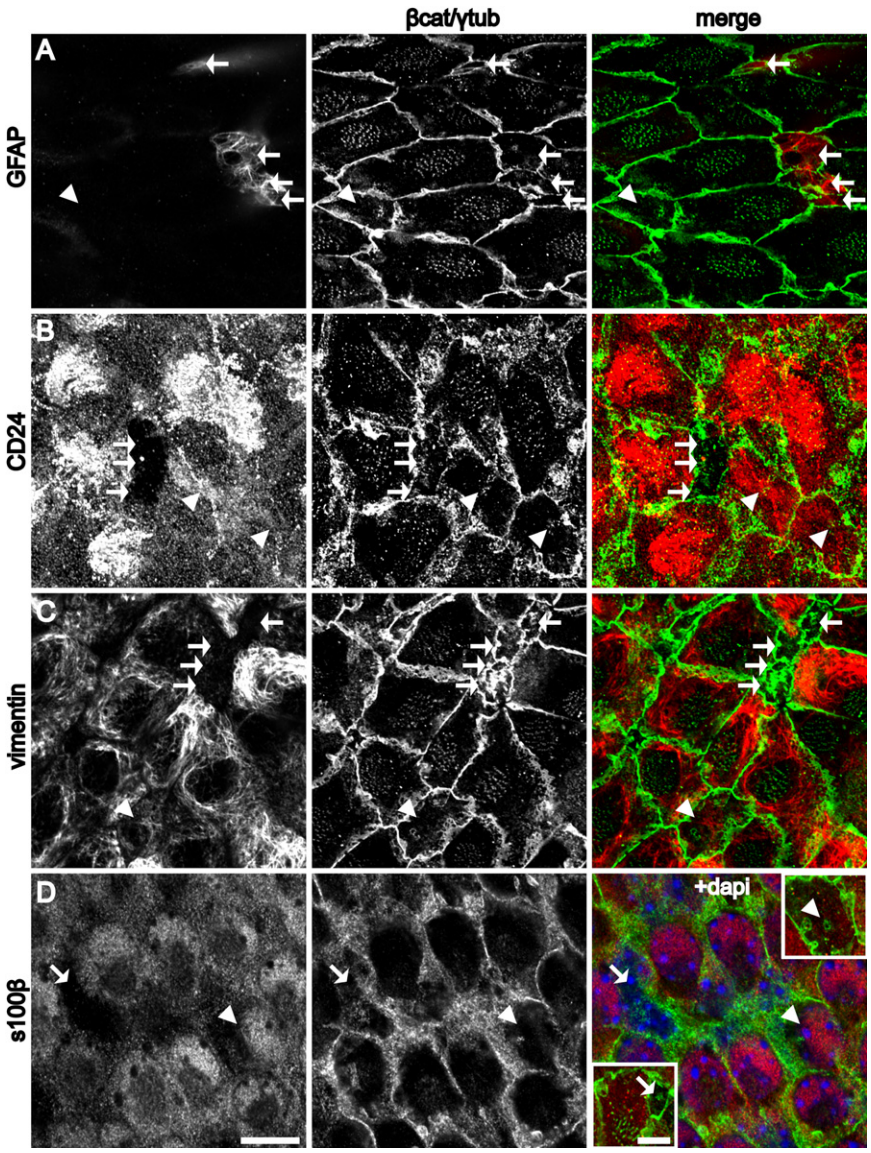

Figure 2. Complementary Expression Patterns of Molecular Markers at the Apical Surface of B1 and E1/E2 Cells

([A]–[C] and [D] insets) Confocal images were taken at the surface of the whole mount and (D) just below the surface. B1 cells (arrows) and E2 cells (arrowheads). (A) GFAP staining is present in B1, but not E1 or E2 cells. (B) CD24 is expressed in the cilia and on the apical surface of E1 and E2, but not B1 cells. (C) Vimentin is expressed at the apical surface of E1 and E2, but not B1 cells. (D) S100β expression is observed in the cell body of E1 and E2, but not B1 cells. Insets show the apical surface of the indicated B1 and E2 cells. Scale bar, 10 μm (A–D). (Inset) Scale bar, 5 μm.

feature of E2 cells was the complex set of electron dense particles surrounding the basal body. By correlative TEM, we confirmed the ultrastructural properties of E1 (Figure 1H) and B1 cells (Figure 1G) (Doetsch et al., 1997).

Surprisingly, we found that B1 cells with a ventricle-contacting apical surface were not rare: we counted 6225 on the lateral wall of one LV in a single, untreated adult mouse (Figures 5A and 5B). These B1 apical surfaces were often found clustered with one another. When quantified, the number of B1 cells was nearly one-third (31.0%) of all cells touching the LV wall (Figure 1I). This finding is in contrast to the conventional view that the walls of the adult ventricular system are lined by a monolayer of ependymal cells (Bruni et al., 1985). However, it is now evident why B1 cells were previously difficult to find by TEM. While they were substantial in number, the average size of the apical surface of a B1 cell was 24.1 μm^2, compared to 265.0 μm^2 for an E1 cell (Figure 1J). Additionally, the average size of the primary cilium of a B1 cell was 3.2 μm, compared to 11.5 μm for E1 cilia (Figure 1K).

B1 and E1/E2 Cells Have Complementary Expression Patterns of Molecular Markers at Their Apical Surfaces

The small apical surfaces of B1 cells could be distinguished from the apical surfaces of E1 and E2 cells by GFAP staining (Figure 2A). These small apical surfaces contained a single basal body. In serial confocal optical sections, GFAP+ B1 apical terminations were associated to cell bodies in the SVZ that had additional basal processes (see below). The GFAP staining, ultrastructure, and cell body location within the SVZ further identified these cells as B1 cells. E1 cells were GFAP− but were CD24+, a marker of ependymal cells (Calaora et al., 1996). Interestingly, E2 cells were also CD24+ (Figure 2B). Vimentin also marked the apical surface of both E1 and E2 cells, but not B1 cells (Figure 2C). Finally, S100β, although it was not strongly expressed at the apical surface, was found to be expressed in the cell body of both E1 and E2 cells, but not B1 cells (Figure 2D). Triple labeling confirmed that B1 cells were GFAP+/S100β−/CD24− (Figure S4A).

B1 Cells Confer Unique Pinwheel Architecture to the Ventricular Surface in Neurogenic Regions of the Adult Brain

We used γ-tubulin and β-catenin staining of the ventricular surface to compare the cellular profiles on neurogenic versus non-neurogenic adult ventricular walls. Adult neurogenesis occurs throughout most of the lateral wall of the LV and part of the anterior medial wall overlying the septum, but not in the caudal medial wall or the third ventricle. While E1 and E2 cells were found in all regions examined, B1 apical surfaces were found only on the lateral wall and in the anterior medial wall of the LVs, coinciding with the neurogenic niche in the adult brain (Figure 3).

In the neurogenic niche, the presence of B1 apical surfaces influenced the geometry of E1 apical surfaces and conferred

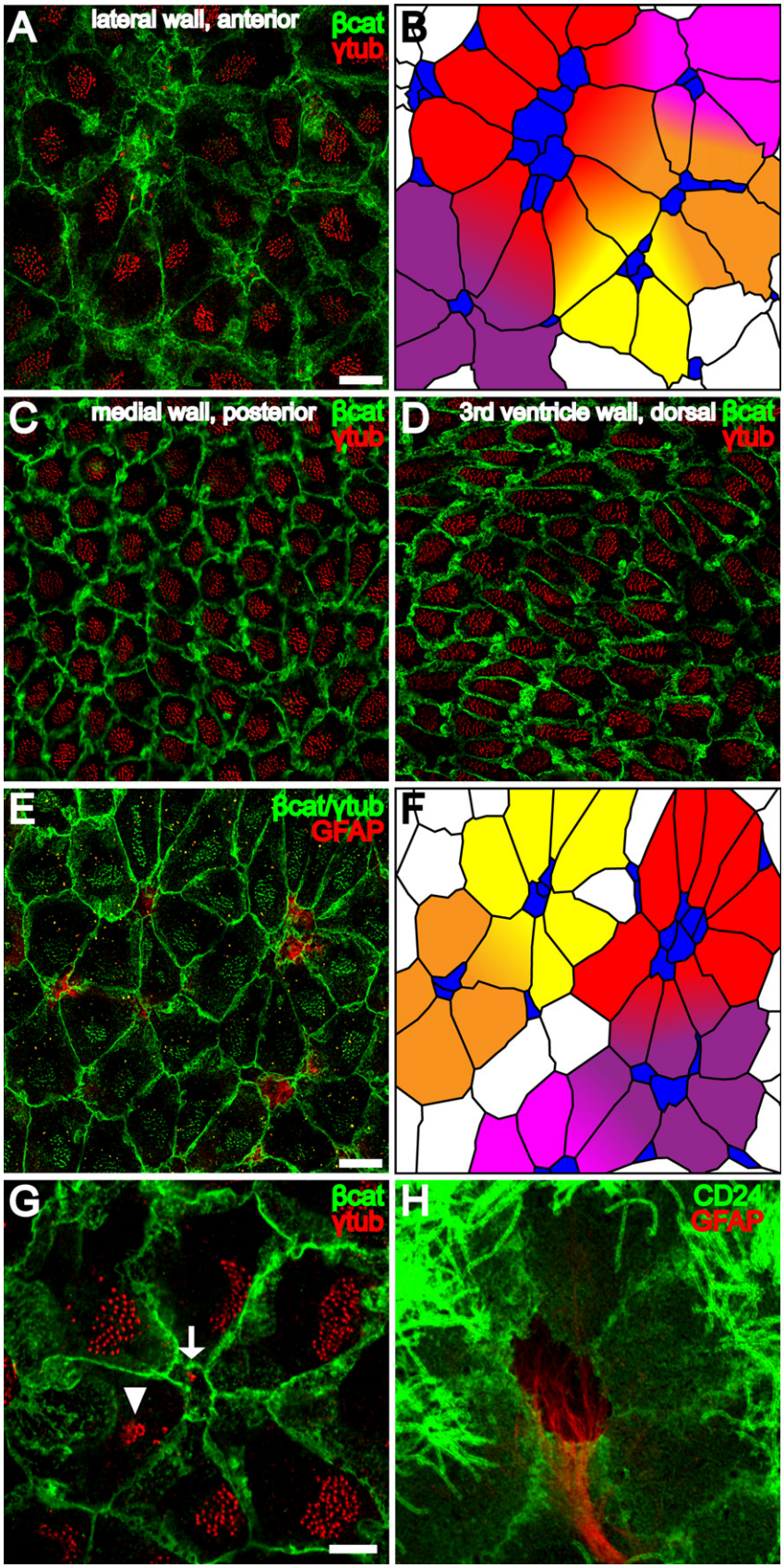

Figure 3. Pinwheel Architecture of the Ventricular Surface in the Adult Neurogenic Niche

(A) Confocal image of the surface of the lateral wall of the LV stained for γ-tubulin (red) and β-catenin (green) reveals pinwheels with centrally located B1 apical surfaces surrounded by ependymal cells. Scale bar, 10 μm (A–D).

(B) Tracing of the β-catenin+ membranes in (A) and color coding of B1 cells (blue) and E1 cells (yellow, orange, red, purple, and magenta) to illustrate five pinwheels. Some E1 cells occupy positions in more than one pinwheel.

(C and D) Neither B1 apical surfaces nor pinwheels are observed in the posterior medial wall of the LV or in third ventricle walls.

(E) Confocal image of the surface of the lateral wall of the LV shows that pinwheels surround GFAP+ (red) B1 cells. β-catenin and γ-tubulin are in green. Scale bar, 10 μm.

(F) Color-coded tracing of the image in (E).

(G) Confocal image demonstrating the diamond shape of E1 apical surfaces found in pinwheels. The polarized position of the basal body patch, found on the right side of each E1 surface in this image, is independent of the E1 surface geometry. A B1 apical surface is indicated in the center of the pinwheel (arrow) and an E2 apical surface (arrowhead) on the periphery. Scale bar, 5 μm (G and H).

(H) Pinwheel architecture revealed by GFAP and CD24, which label B1 and E1/E2 cells, respectively.

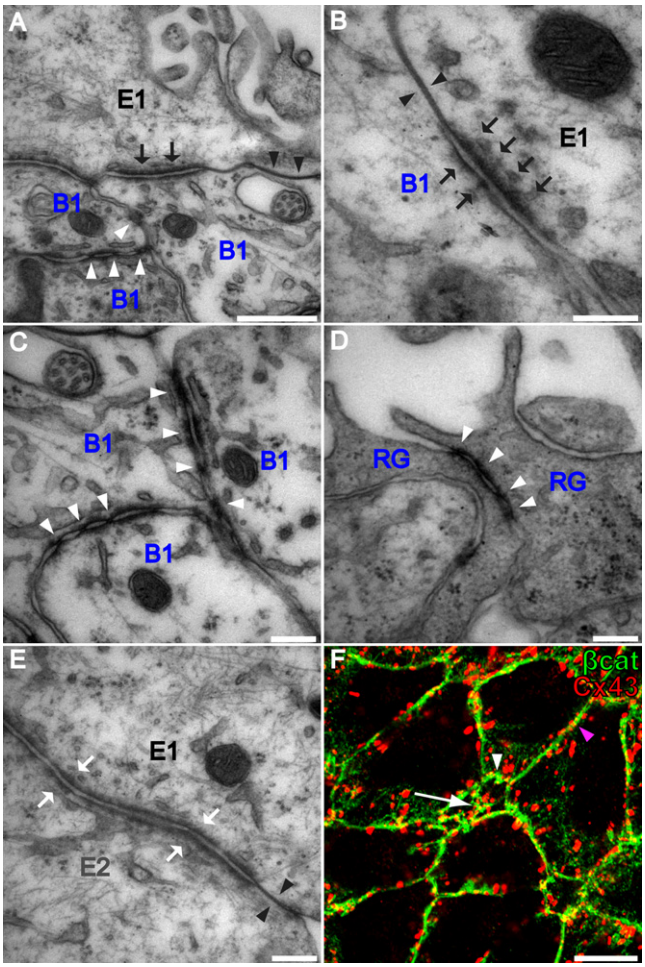

Figure 4. Apical Intercellular Junctional Complexes Differ at B1-B1, B1-E1, and E1-E2 Junctions

(A) In addition to tight junctions (black arrowheads), B1 and E1 cells form asymmetric adherens junctions (black arrows). B1 cells form symmetric atypical adherens junctions with each other (white arrowheads). Scale bar, 500 nm.

(B) Higher magnification of an asymmetric B1-E1 adherens junction (black arrows) and a B1-E1 tight junction (black arrowheads). Scale bar, 200 nm.

(C) Higher magnification of atypical B1-B1 adherens junctions. Scale bar, 200 nm.

(D) Radial glia (RG) in the neonatal VZ have apically localized symmetric atypical adherens junctions (white arrowheads) similar to those at B1-B1 junctions in the adult. Scale bar, 200 nm.

(E) E1 and E2 cells form tight junctions (black arrowheads) and symmetric adherens junctions (white arrows) indistinguishable from those at E1-E1 junctions. Scale bar, 200 nm.

(F) Confocal image of the surface of the lateral wall of the LV stained for Cx43 (red) and β-catenin (green) reveals that gap junctional components are present at B1-B1 (arrow), B1-E (white arrowhead), and E-E (magenta arrowhead) intercellular membranes. Scale bar, 10 μm.

a striking architecture to the ventricular wall (Figures 3A, 3B, 3E, and 3F). The apical surface of one or more B1 cells was surrounded by E1 cells in a specific pattern. The pattern, which resembles a pinwheel (Figure 3G), appeared to maximize the packing of E1 cells around the B1 apical surface. The shape of each E1 apical surface approximated a diamond with one vertex contacting the B1 apical surface. The resulting pinwheel pattern was only observed on the ventricular surface in neurogenic regions, where B1 cells were found (Figures 3A, 3B, and 3E–3H), and not in nonneurogenic regions, where E1 apical surfaces were more regularly shaped (Figures 3C and 3D). Pinwheels were also observed using antibody staining to ZO1, a component of apical junctional complexes that provided a sharper delineation of cell boundaries (Figure S5A). The core of the pinwheels was also evident with GFP staining of whole mounts from Aldh1L-GFP BAC transgenic mice (Figure S5B). Aldh1L has been shown to be enriched in astrocytes (Cahoy et al., 2008), and the regulatory region of this gene has been used to drive GFP expression in astrocytes in a BAC transgenic mouse (GENSAT project).

A high magnification of one pinwheel is shown in Figure 3G. In addition to their striking radial organization, E1 cells have planar polarity that underlies the directional beating of motile cilia to propel cerebrospinal fluid (Sawamoto et al., 2006). The basal body patch in each E1 cell is found downstream with respect to the direction of ciliary beating (Z.M. and A.A.-B., unpublished data). Interestingly, the geometry and radial polarity of E1 apical surfaces found in pinwheels appeared to be independent of the planar polarity of their basal body patch.

The peripheral packing of E1 cells around central clusters of B1 cells suggested that these cells may have specialized intercellular junctions at their apical surfaces. EM analysis of the apical junctional complexes between the various combinations of cell types (B1-B1, B1-E1, E1-E1, and E1-E2) revealed that B1-B1 and B1-E1 junctions were unique (Figure 4). For this analysis we used serial section reconstruction at the EM to confirm cell identity based on the number of cilia each cell had. B1-B1 junctions (white arrowheads in Figures 4A and 4C) had symmetric discontinuous adherens junctions with periodic electron-dense deposits at sites where membranes became tightly opposed or pinched. Interestingly, these junctions were very similar to those observed between radial glia in the neonatal VZ (Figure 4D). Short stretches of tight junctions were occasionally observed between B1 cells. E1-E2 junctions were symmetric; both tight (black arrowheads in Figure 4E) and adherens junctions (white arrows in Figure 4E) were observed, and these junctions were indistinguishable from those observed between E1 cells. Interestingly, B1-E1 junctions (Figure 4B) included both tight and adherens junctions, but the latter were asymmetric. More electron-dense material was accumulated inside the membrane on the E1 side than on the B1 side (black arrows in Figure 4B). Gap junctions cannot be reliably detected by TEM. We therefore stained the LV wall of adult mice with antibodies that recognize gap junction subunit Connexin 43. Dotted staining was observed at the interface of B1-B1, B1-E, and E-E cells (Figure 4F). While we do not know whether these cells are functionally coupled, the above observation suggests that Connexin 43 is not unique to particular junctional complexes between the three cell types contacting the ventricle. Instead, the above results suggest that it is the adherens junctions that characterized these homotypic and heterotypic adhesions between the different cell types at their apical intercellular boundaries.

Surface Maps of the LV Walls Reveal Hot Spots of B1 Cells

The above analysis showed that B1 cells were limited to neurogenic regions of the adult ventricular system but did not show the

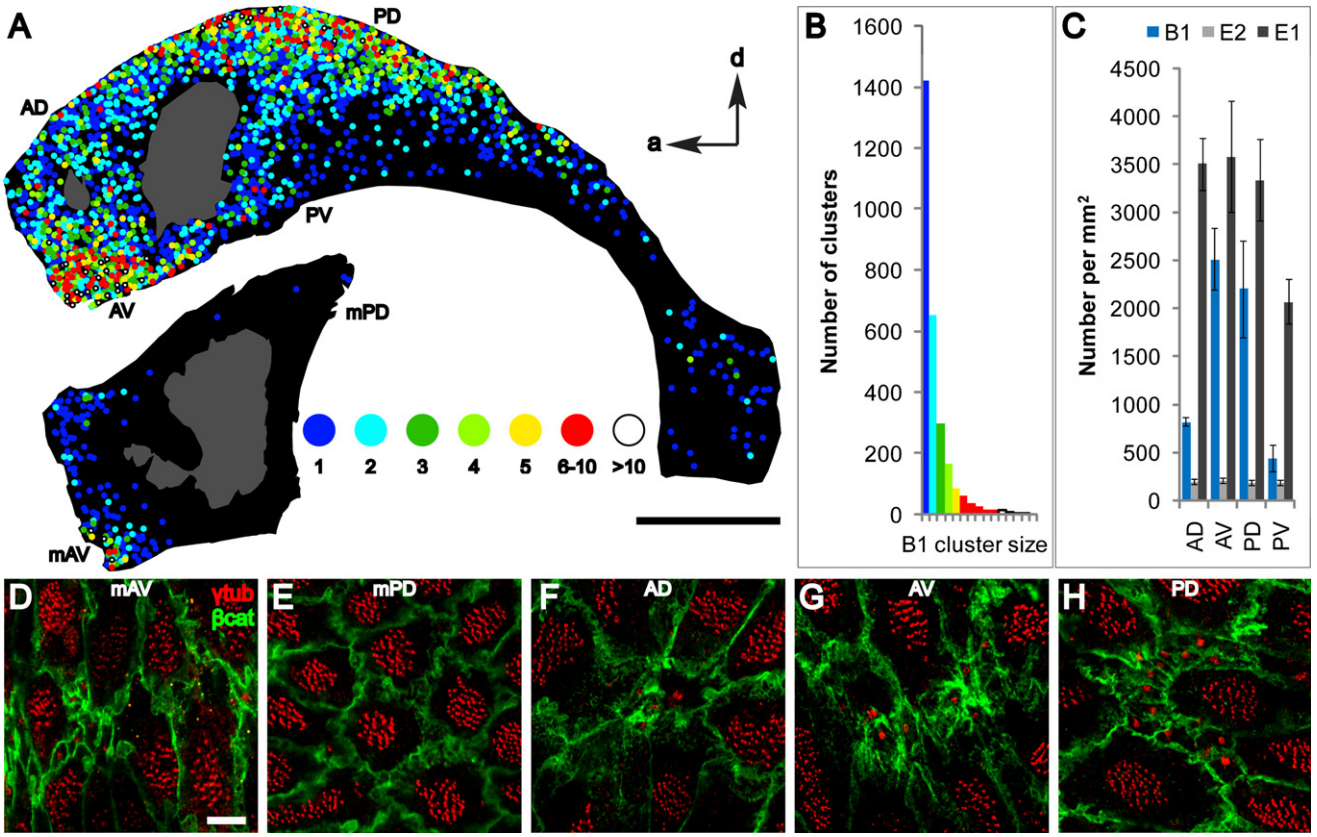

Figure 5. Surface Maps of the Walls of the LV Reveal Hot Spots of B1 Apical Surfaces

(A) The position of B1 apical surfaces is indicated on the maps by color-coded circles depicting the number of B1 apical surfaces per cluster (1 to >10 cells per cluster). Hot spots were found in anterior-ventral (AV) and posterior-dorsal (PD) regions of the lateral wall and anterior-ventral (mAV) region of the medial wall. The adhesion point between lateral and medial walls is shown in gray. Scale bar, 1 mm.

(B) Distribution of B1 cluster size.

(C) Density of B1, E1, and E2 apical surfaces in four regions of the lateral wall in three animals. Regions quantified are indicated in (A) and Figure S13. Error bars show SEM.

(D–H) Representative confocal images from different regions of the surface of the lateral and medial walls stained for γ-tubulin and β-catenin. Scale bar, 5 μm.

distribution within the neurogenic regions. To create a comprehensive map of the location of B1 cells on the walls of the LV, we reconstructed the entire surface of one lateral wall and the anterior portion of one medial wall stained with γ-tubulin and β-catenin. These surface maps were reconstructed from a series of 222 (lateral wall) and 106 (medial wall) tiled, high-power confocal fields (212 × 212 μm^2/field).

B1 cells with ventricle-contacting apical surfaces were found throughout the lateral wall (Figure 5A) in clusters of 1–40 cells. We quantified the number and position of B1 apical surfaces in the different regions of the lateral and anterior medial wall of the LV. This data was color-coded to indicate clusters of 1, 2, 3, 4, 5, 6–10, or >10 B1 apical surfaces. B1 apical surfaces were more concentrated in two hot spots, in the anterior-ventral and posterior-dorsal regions. B1 apical surfaces were also found in the most anterior aspect of the medial wall of the LV (Figure 5A). This region has recently been found to contain neurogenic precursors that generate specific subpopulations of olfactory bulb neurons in the postnatal rodent brain (Merkle et al., 2007). This is consistent with the idea that ventricle-contacting B1 cells function as progenitor cells and shows that the presence of B1 apical surfaces is an indicator of neurogenic ventricular walls in the adult.

Next, we quantified the number of B1 apical surfaces in four different lateral wall regions from three more animals (Figure 5C). We consistently found that the anterior-ventral and posterior-dorsal regions had the highest number of B1 apical surfaces, with 2515 and 2206 per mm^2, respectively (Figures 5G and 5H). The anterior-dorsal region had fewer, with 823 (Figure 5F), and the posterior-ventral region had the fewest with 442 B1 apical surfaces per mm^2. In contrast, the density of E1 cells was similar among the regions (3343–3584 per mm^2), except in the posterior-ventral region (2072 per mm^2), where E1 cells had a larger surface area. E2 cells were found in similar numbers throughout the different regions (185–211 per mm^2).

B1 Cells Have a Long Basal Process Similar to Their Radial Glial Progenitors

To understand how specialized apical endings on the ventricular surface relate to the architecture of the SVZ, we used whole-mount staining and confocal microscopy to look beneath the ventricular surface and ependymal layer. One striking result

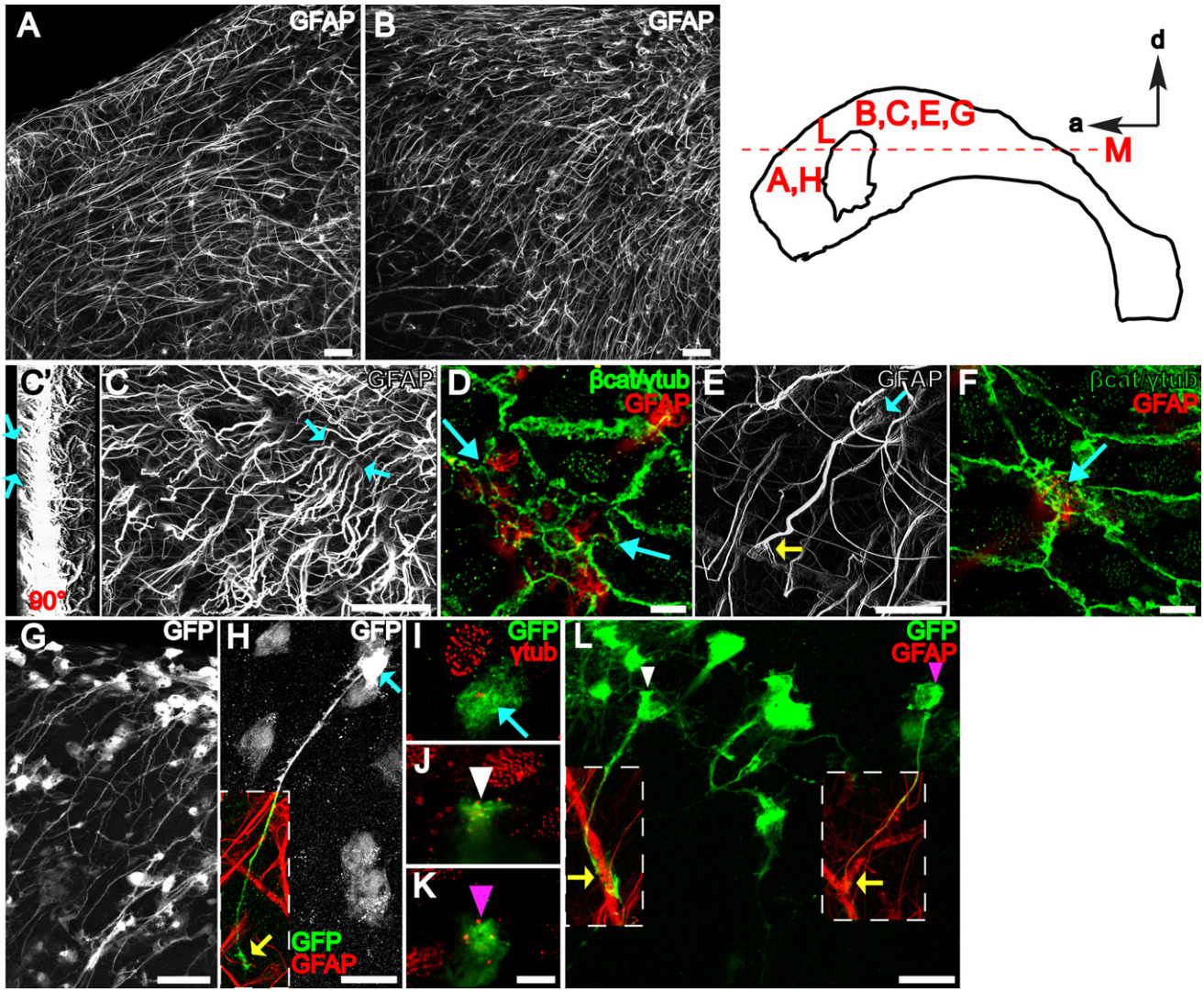

Figure 6. B1 Cells with an Apical Ventricular Contact Have a Long Basal Process Terminating on Blood Vessels

The diagram of the lateral wall at the top right indicates where the images were taken.

(A and B) Z projections of confocal stacks (50 μm thick) taken from whole mounts stained for GFAP. Because whole mounts are freshly dissected, secondary antibodies used against mouse anti-GFAP primary antibody also stain blood vessels that contain endogenous mouse IgGs. Scale bar, 50 μm.

(C) Z projection of a higher-power confocal stack (50 μm thick) taken from a whole mount stained for GFAP. Blue arrows indicate the apical endings of long GFAP+ processes. Scale bar, 50 μm. (C′) Three-dimensional reconstruction of the stack in (C) rotated 90°. Blue arrows indicate processes reaching the ventricular surface and correspond to blue arrows in (C).

(D) Confocal image of the surface (costained for γ-tubulin and β-catenin in green) in the region between the blue arrows in (C) reveals that the apical endings indicated in (C) belong to a group of 11 B1 cells with GFAP+ apical surfaces on the ventricle. Scale bar, 5 μm.

(E and F) The long basal process of a B1 cell with an apical ventricular contact (blue arrows) terminates on a blood vessel forming an endfoot (yellow arrow in [E]). Scale bar, 25 μm (E) and 5 μm (F).

(G) B1 cells with apical ventricular contact could be labeled by adeno-GFAPp:Cre virus injected into the LV of Z/EG mice. Scale bar, 50 μm.

(H) High-power confocal Z stack projection reveals the complete morphology of a B1 cell: apical contact with the ventricle (blue arrows in [H] and [I]) and basal contact with blood vessels (yellow arrow in [H]). Scale bar, 25 μm.

(I–K) Confocal images of the ventricle-contacting apical surface of B1 cells corresponding to the color-coded arrow in (H) and arrowheads in (L). Scale bar, 5 μm.

(L) Adult B1 cells are derived from neonatal radial glia. Note the apical ventricular contact (white and magenta arrowheads in [J]–[L]) of two GFP+ B1 cells derived from neonatal radial glial labeling. Both cells have a long basal process contacting a blood vessel (yellow arrows). Scale bar, 25 μm.

was the presence of very long GFAP+ fibers throughout the lateral wall of the LV. These fibers were oriented in different directions depending on location (Figures S6 and S7). Figures 6A and 6B show that most GFAP+ fibers found in the anterior-dorsal lateral wall of LV were oriented tangentially to the surface and ran anteriorly. Fibers found more ventrally were oriented tangentially to the surface but ran ventrally (Figure 6B).

To determine whether these fibers belonged to B1 cells with apical surfaces on the ventricle, we used high-power confocal stacks to image a block 50 μm deep of the lateral wall in whole

mounts stained for GFAP, γ-tubulin, and β-catenin. At the ventricular surface, we observed GFAP+ B1 apical endings as before (Figure 6D), but tracing the GFAP+ fibers deeper revealed that they extended for a long distance (Figure 6C, arrows indicate apical endings shown in Figure 6D). The thick bundle of GFAP+ intermediate filaments that comprised the long basal process frayed into many thinner bundles closer to the apical surface (Figures 6E and 6F, blue arrow). To quantify the proportion of long GFAP+ processes that made apical contact with the ventricle, we traced individual fibers in confocal stacks. We found that almost all cells (98%, 227 of 232 cells from n = 3 mice) identified by their long GFAP+ basal process made apical ventricular contact. At the other end of this basal process, we observed that 96% (134 of 139, n = 3 mice) of GFAP+ basal processes terminated in an endfoot on a blood vessel (Figure 6E, yellow arrow). GFAP+ B1 cells with an apical surface on the ventricle and a long basal process were observed at all ages tested (up to 9 months old, data not shown). Chains of migrating neuroblasts in the SVZ are ensheathed by gliotubes that run parallel to the orientation of the chains (Lois et al., 1996; Peretto et al., 1997). Double staining for GFAP to label B1 cells and doublecortin to label chains of migrating cells showed that B1 basal processes contribute to the gliotubes. Basal processes of B1 cells wrapped around the chains and then ran parallel to the orientation of these chains for some distance before terminating on blood vessels (Figure S8). Beneath the layer of GFAP+ B1 cells' long processes, there was a layer of scattered astrocytes with multipolar morphology revealed by GFAP staining (Figure S9A). These cells correspond to B2 cells previously described (Doetsch et al., 1997). Multipolar astrocytes were also observed beneath the ependyma in nonneurogenic regions such as the third ventricle (Figure S9B).

Based on correlative TEM, we suspected that GFAP staining did not reveal the complete morphology of B1 cells. Consequently, we injected an adenovirus expressing Cre under the GFAP promoter (Merkle et al., 2007) into the LV of Z/EG mice (Novak et al., 2000), a Cre reporter line expressing GFP. This technique provided a way to label B1 cells, which have both a ventricle-contacting apical surface (allowing infection via the ventricle) and an active GFAP promoter (allowing Cre expression from the adenovirus). We then reconstructed high-power confocal stacks of labeled B1 cells filled with GFP (Figures 6G–6I). Most B1 cell bodies were located immediately underneath ependymal cells, with a very short apical process extending between ependymal cells to make contact with the ventricle (Figures 7E and 7F and 7E′ and 7F′). In some cases, rather than extending an apical process, it appeared that part of the B1 cell body was squeezed between ependymal cells to make direct contact with the ventricle (Figures 6H and 6I). A very long process emanated from the basal side of the cell body and extended tangentially, ending with an endfoot on a blood vessel (Figure 6H, yellow arrow). In addition, B1 cells had lateral lamellar extensions of membrane from their cell body (like a fried egg) that spread across the basal side of adjacent ependymal cells. While these lateral extensions appeared as individual processes in sections (Doetsch et al., 1997), the whole-mount analysis revealed that many of these processes were part of a continuous thin sheet of membrane spanning in all directions away from the cell body. Several smaller processes were also observed emanating from the cell body and the proximal part of the long basal process.

The morphology of B1 cells was reminiscent of radial glia of the embryonic VZ. Radial glia have a short, ventricle-contacting apical process and a very long, pial-contacting basal process. This long basal process can be used to specifically label radial glia by injecting an adenovirus expressing Cre into the striatum of neonatal Z/EG mice. This method was used to determine that B cells in the adult SVZ are derived from radial glia (Merkle et al., 2004). To determine if the radial glia-derived B cells identified in the Merkle et al. study correspond to B1 cells we identified above, we performed the same radial glial targeting in neonatal Z/EG mice, sacrificed the animals 2 months later, and prepared whole mounts. We observed B1 cells as before. Figure 6L shows two of these B1 cells, each with a short apical process contacting the ventricle (Figures 6J and 6K) and a long basal process distally wrapped around a blood vessel. B1 cells derived from radial glia also exhibited the lateral lamellar extensions of membrane cupping the basal side of adjacent ependymal cells (Figures S10A and S10B). In addition, we traced, using a camera lucida, the fine details of eight B1 cells with apical contacts in 50 μm horizontal sections, where it was more common to see more of the basal process (Figure S10C). In sharp contrast to the morphology of B1 cells, typical astrocytes elsewhere in the adult brain, including some found in the SVZ (B2 cells), were multipolar, with bushy, highly branched processes (Figure S11). This is consistent with previous work showing that dividing GFAP-expressing progenitors in the adult SVZ have a simple morphology compared to differentiated multipolar parenchymal astrocytes (Garcia et al., 2004).

The above results labeling adult SVZ B1 cells by multiple approaches showed that these cells have two epithelial compartments: (1) apical, in contact with the ventricle, and (2) basal, in contact with blood vessels. In our previous ultrastructural reconstructions, we had missed these basic features of adult SVZ NSCs (Doetsch et al., 1997). Both these compartments are very difficult to identify in thin sections: the apical ending is very small and frequently connected by a thin neck with the cell body, which may lie in an entirely separate section. It is therefore not surprising that B1 cells contacting the ventricle were only rarely observed (Doetsch et al., 1999b). Our previous work identified many small profiles of B cells deep in the SVZ. However, as illustrated in the current analysis, the basal processes can run tangentially for several hundred microns, making it difficult, if not impossible, to link these small profiles of basal processes with their cell bodies using serial sections.

Ventricle-Contacting B1 Cells Undergo Mitosis and Are Neurogenic

The above observations indicated that GFAP-expressing SVZ B1 cells, which correspond to the adult NSCs, contact the LV. Apical processes of B1 cells were nestin+ (Figure S4B), and 29% (26 of 89, n = 2 mice) were positive for CD133 (Figures S4C and S4D), both markers of NSCs (Uchida et al., 2000). A recent study suggests that CD133+/CD24− cells in contact with the ventricle are adult NSCs (Coskun et al., 2008). In our study, 100% (720 of 720, n = 2 mice) of E1 and E2 cells expressed CD24, while none of the B1 apical endings expressed this marker. This suggests that CD133+/CD24− cells identified in

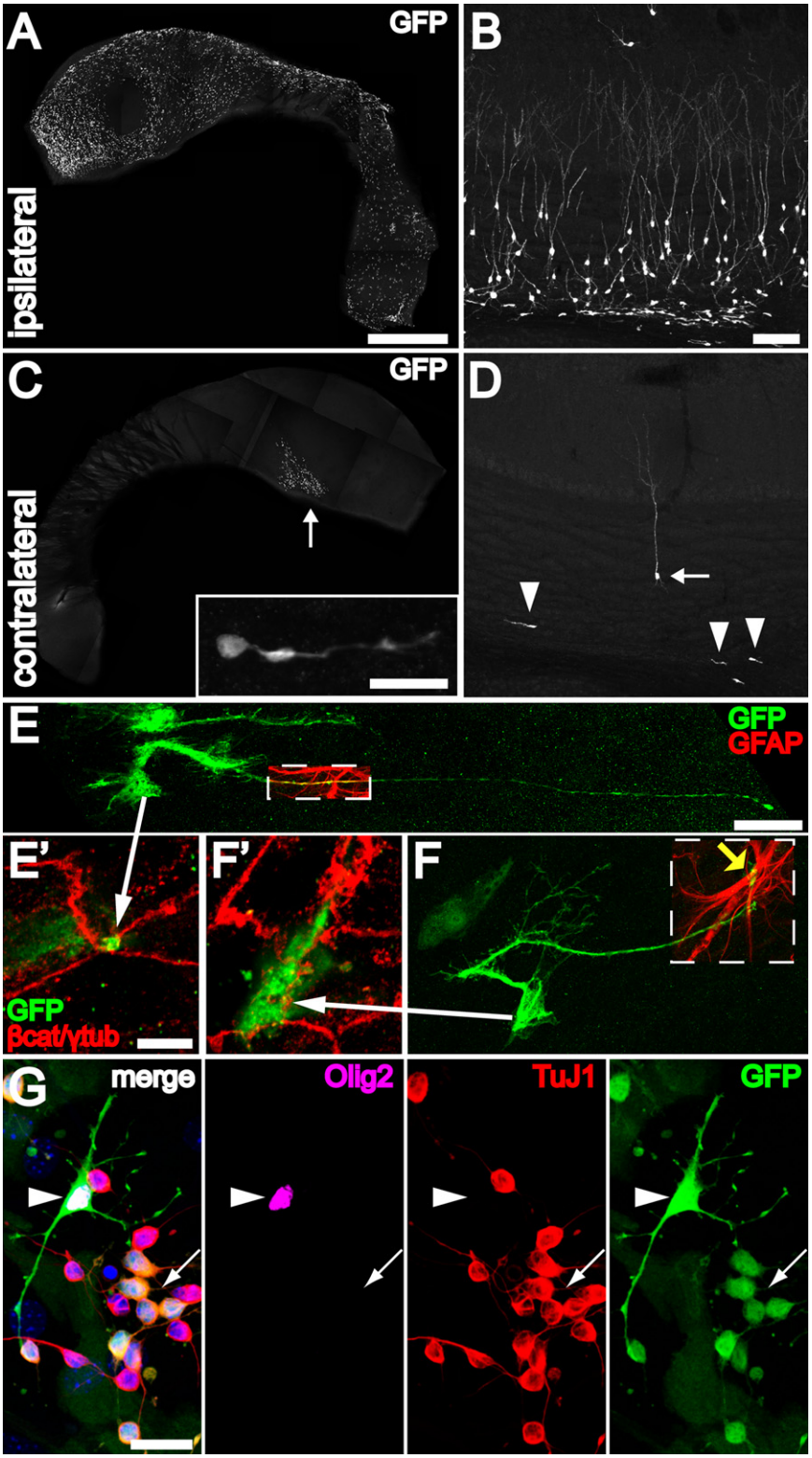

Figure 7. B1 Cells with Apical Ventricular Contact Are Neurogenic In Vivo and Differentiate into Neurons, Astrocytes, and Oligodendrocytes In Vitro

(A) Injection of adeno-GFAPp:Cre into one LV of Z/EG mice results in many labeled ventricle-contacting B1 cells on the ipsilateral lateral wall. The whole-mount images (A and C) were reconstructed from low power (1.3 × 1.3 mm) tiled confocal images. Scale bar, 1 mm (A and C).

(B) Thirty days after injection, many labeled neurons and neuroblasts can be found in the ipsilateral olfactory bulb. Scale bar, 100 μm (B and D).

(C) Virus that backfills the contralateral LV labels a few ventricle-contacting B1 cells on the contralateral side. Most of these labeled cells are close to the foramen of Monro (arrow). These labeled B1 cells give rise to neuroblasts (inset) in the contralateral SVZ, examined 30 days after injection. (Inset) Scale bar, 20 μm.

(D) The few labeled ventricle-contacting B1 cells on the contralateral side gave rise 30 days later to neuroblasts (arrowheads) and neurons (arrow) in the contralateral OB.

(E and F) B1 cells in the contralateral lateral wall have characteristic features of apical ventricular contact (arrows to [E′] and [F′]), GFAP expression (boxed regions), and a long basal process with endfeet on blood vessels (yellow arrow). Scale bar, 25 μm. (E′ and F′) Confocal images of the ventricle-contacting apical surface of B1 cells in (E) and (F). Scale bar, 5 μm.

(G) GFP-labeled B1 cells dissected from the contralateral wall could be passaged and differentiated in vitro into TuJ1+ neurons (arrow), Olig2+ oligodendrocytes (arrowhead), and adherent GFAP+ (data not shown) astrocytes. Scale bar, 20 μm.

this previous paper correspond to ventricle-contacting B1 cells. Using sections of the walls of the LVs, previous studies failed to find dividing ependymal cells (Spassky et al., 2005). Here, we stained whole mounts for γ-tubulin and β-catenin to identify B1 apical surfaces and phosphohistone H3 (PH3) to identify cells in mitosis or Ki67 to identify proliferating cells (BrdU staining was not reliable; required HCl pretreatment decreased β-catenin staining at the surface). We serially reconstructed with the confocal microscope 91 PH3 or Ki67+ B1 cells (n = 3 mice) contacting the ventricle (Figure S12). In all cases, the mitotic soma from these ventricle-contacting B1 cells remained squeezed basally by neighboring ependymal cells. Figure S12A shows a B1 apical surface that is PH3+. Following the confocal stack deeper into the tissue revealed that this PH3+ cell was in anaphase, with one of the sister chromatids (yellow arrow) just beneath the apical membrane and the other (magenta arrow) deeper in the SVZ, beneath an ependymal cell. This and another cell shown in Figure S12F appear to be dividing asymmetrically. Interestingly, Ki67 expression is cell-cycle phase dependent (Scholzen and Gerdes, 2000), and we observed Ki67+ B1 cells in all phases

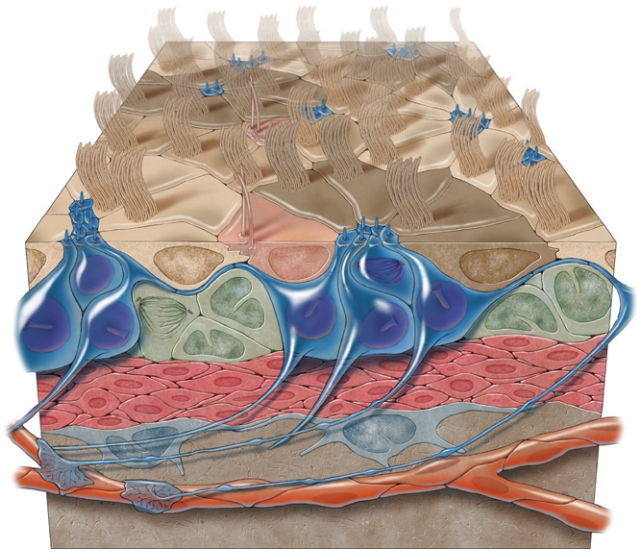

Figure 8. Three-Dimensional Model of the Adult VZ Neurogenic Niche

Three-dimensional model of the adult VZ neurogenic niche illustrating B1 cells (blue), C cells (green), and A cells (red). B1 cells have a long basal process that terminates on blood vessels (orange) and an apical ending at the ventricle surface. Note the pinwheel organization (light and dark brown) composed of ependymal cells encircling B1 apical surfaces. E2 cells are peach.

(Figure S12). We found no evidence of E1 or E2 cells labeled by Ki67, PH3, or BrdU.

To test whether B1 cells with a ventricular contact are neurogenic, we injected adeno-GFAPp:Cre into one LV of Z/EG mice. To ensure that we were tracing the fate of only those B1 cells labeled via their ventricle-contacting surface, we focused our analysis on the contralateral side. Labeling on the contralateral side could only occur through viral diffusion from the ventricular system, and this was confirmed by the pattern of labeling close to the foramen of Monro (arrow in Figure 7C). Labeled B1 cells in the contralateral whole mount had an apical surface on the ventricle (Figures 7E′–7F′) and a long basal process ending on a blood vessel (Figures 7E and 7F). Labeling B1 cells contacting the LV in this manner resulted in labeled neuroblasts in the contralateral SVZ (Figure 7C, inset), and labeled neuroblasts and neurons in the contralateral olfactory bulb in six of six animals (Figure 7D). This shows that B1 cells labeled via their apical surface produce neurons and neuroblasts up to 1 month after labeling. We also microdissected the contralateral SVZ 2 days after unilateral injection of adeno-GFAPp:Cre and plated dissociated cells as previously described (Scheffler et al., 2005). GFP+ cells from the contralateral side could be passaged and generated large colonies of Tuj1+ cells. These cultures also generated many GFP+ adherent GFAP+ astrocytes and a few Olig2+ oligodendrocytes (Figure 7G). These data indicated that B1 cells labeled via their ventricle-contacting apical surface are capable of generating large numbers of neurons in vivo and in vitro.

DISCUSSION

Here we uncovered an architecture for the germinal layer of the adult brain LV, revealing its pinwheel organization and the presence of biciliated ependymal cells with unique basal bodies. The work, summarized in the illustration in Figure 8, suggests that B1 cells maintain a modified neurogenic VZ in the adult mouse brain.

E2 Cells: An Ependymal Cell

E2 cells were ultrastructurally similar to E1 cells and had long (9 + 2) cilia. The most distinctive feature of E2 cells was their large basal body (Figure 1F). Multiple studies have described the ultrastructure of ependymal cells (Bruni et al., 1985; Flament-Durand and Brion, 1985; Del Brio et al., 1991), but to our knowledge, this basal body organization has not been observed before. E2 cells comprised less than 5% of cells on the ventricular surface and had only two cilia. Therefore, their contribution to CSF flow is likely minute. They were not observed in division and were present in nonneurogenic regions like the third and fourth ventricles (Z.M. and A.A.-B., unpublished data), making it unlikely that they function as progenitors. Interestingly, unlike E1 cells, the cilia of E2 cells were partially invaginated (Figure 1E). Primary cilia, which are also partially invaginated (Sorokin, 1968) (Figure 1G), function as transducers for cell signaling pathways including Shh (Huangfu et al., 2003; Corbit et al., 2005) and Wnts (Gerdes et al., 2007). The basal body and pericentriolar region appears to play an important role in the signaling function of primary cilia (Gerdes et al., 2007; Rohatgi et al., 2007). E2 cells and their cilia may serve as mechanical or chemical sensors for CSF flow or composition (Bruni et al., 1985). The elaborate basal body of E2 cells may be involved in transmitting information between the ciliary axoneme and other intracellular compartments.

B1 Cells Retain a Long Basal Process

During earlier development, neuroepithelial cells and radial glia bridge between the ventricular and the subpial surfaces; signals arising at both poles are essential for proper germinal activity (e.g., ventricular: Bittman et al. [1997]; Nadarajah et al. [1997]; Kosodo et al. [2004], and Weissman et al. [2004]; e.g., subpial: Halfter et al. [2002]; Haubst et al. [2006]). Radial glia establish specialized endings with blood vessels (Misson et al., 1988; Noctor et al., 2001). In the subgranular zone of the adult hippocampal dentate gyrus, NSCs reside in close proximity to blood vessels (Palmer et al., 2000). It has been suggested that extracellular matrix (Mercier et al., 2002) and soluble factors (Leventhal et al., 1999; Shen et al., 2004) secreted by blood vessels play important roles in regulation of adult neurogenesis. In the present study, we found that the long basal process of B1 cells terminated directly on blood vessels forming specialized endfeet. B1 cells are derived from radial glia and their basal processes are likely remnants of radial glial fibers. Basal processes and their contacts with the vasculature may allow B1 cells to respond to signals in the perivascular extracellular matrix (Kerever et al., 2007) or to hormones or growth factors present in the circulation, such as prolactin (Shingo et al., 2003), PDGF (Jackson et al., 2006), or IGFs (Jiang et al., 1998).

Radial glia of the developing neocortex (Rakic, 1972) and radial cells in songbirds (Alvarez-Buylla and Nottebohm, 1988) use the long basal process to maintain contact with neuronal progeny during early stages of differentiation and migration. Many of the basal processes of B1 cells wrap around chains of neuroblasts (Figure S8). This arrangement may be important for guiding the migration and maturation of young neurons.

Recent work suggests that chemorepellants in cerebrospinal fluid and its directional flow contribute to directional migration (Sawamoto et al., 2006). We show here that B1 cells bridge these two compartments and could transfer information from the ventricular surface to the SVZ.

B1 Cells Maintain a Modified Ventricular Zone in the Adult Brain

The present results indicate that B1 cells in the adult brain, like radial glia earlier in development, have an apical surface in contact with the ventricle. In adult songbirds (Alvarez-Buylla et al., 1990; Goldman et al., 1996) and reptiles (Garcia-Verdugo et al., 2002), the neural progenitors are also ventricle-contacting radial cells. The present study revealed a center-surround pinwheel organization to this mixed VZ, which has ependymal cells in addition to NSCs. Pinwheels were abundant throughout the neurogenic niche but absent from nonneurogenic ventricular walls. This organization may be fundamental for adult neurogenesis, allowing B1 cells in the core of the pinwheels to (1) contact the ventricular fluid, which may regulate NSC behavior; (2) share apical junctional complexes (gap and adherens junctions) among themselves and with ependymal cells, likely essential for NSC symmetric and asymmetric division (Chenn and Walsh, 2002; Kosodo et al., 2004); and (3) be exposed to apical signals, like Noggin (Lim et al., 2000; Peretto et al., 2004), that are largely derived from ependymal cells. The VZ and pinwheel organization described here provides basic anatomical information to understand B1 cell regulation. It will be interesting to determine how exogenous growth factor stimulation (Cho et al., 2007) may alter, or mimic, apical-basal polarity.

The pinwheel architecture of the adult VZ may also hold clues about how it is derived from the embryonic VZ. As ependymal cells begin to differentiate from radial glia during perinatal development and their apical surfaces expand, they may restrict the space available for neurogenic radial glia, corralling them into central clusters held together by apical junctional complexes. The maintenance of cell-type-specific apical junctional complexes between radial glia at the time of ependymal cell differentiation is likely essential for the development of pinwheels in the adult VZ. This scenario suggests that apical junctions between B1 cells are different than those between ependymal cells or between ependymal cells and B1 cells. This is precisely what we observed (Figure 4). Interestingly, a recent study showed that numb and numb-like are required for maintaining radial glial adherens junctions and that numb overexpression results, in a cadherin-dependent manner, in abnormal maintenance of radial glia postnatally (Rasin et al., 2007). Conditional removal of numb from the neonatal SVZ results in severe disorganization of the ependymal layer that is partially repaired by cells that escaped recombination (Kuo et al., 2006). Numb is likely to play important roles in the development of pinwheels, but this process remains to be studied. The pinwheel pattern also suggests a possible role for lateral inhibition by Notch signaling. In the postnatal hippocampal dentate gyrus, Notch is required for GFAP+ stem cell maintenance, and absence of Notch results in neuronal differentiation (Breunig et al., 2007). Similarly, in the neonatal VZ, Notch-expressing B1 cells may signal to neighbor ependymal cells during their differentiation, resulting in the formation of pinwheels by lateral inhibition.

Injuries to the ependymal cells can result in scars in the ventricular wall that are largely composed of astrocytes (Del Carmen Gomez-Roldan et al., 2008). Recent work suggests that in the aging mammalian brain, a subpopulation of astrocytes can grow multiple cilia (Luo et al., 2008). We have noticed that the number of B1 cells touching the LV decreases significantly with age (Z.M. and A.A.-B., unpublished data). It will be interesting to determine if B1 cells touching the ventricle transform into ependymal-like cells with age or whether these cells actively participate in ependymal repair.

Progenitor cells have been isolated from regions around the LV in the adult human brain (Pincus et al., 1998). Rare SVZ astrocytes were observed with processes extending toward the ventricle (Sanai et al., 2004). It will be interesting to investigate if these cells in humans have apical ventricular contacts and pinwheel organization. The staining methods described here may facilitate the identification of potential neurogenic regions along the adult human ventricular system.

The persistence of an adult VZ leads us to re-examine the roles of the VZs and SVZs in adult neurogenesis. In the embryo, the ventricular and subventricular compartments are largely distinct: the VZ for stem cells and the SVZ for intermediate progenitors (Noctor et al., 2007a). Similarly, the adult neurogenic niche may be comprised of two compartments, a VZ for B1 cells and an SVZ for intermediate progenitors, or C cells, and neuroblasts, or A cells. The distinction between these compartments in the adult may be less clear due to the apical expansion of ependymal cells. Consistently, we show that the cell body of most B1 cells is pushed back toward the SVZ. This provides a unified hypothesis on the roles of the VZ and SVZ in neurogenic niches of the brain, from embryo to adult. The study shows that contact with the ventricular cavity, being part of an epithelium, and having specialized apical structures are germinal niche properties retained by adult NSCs. It is likely that all of these are fundamental to their function. The en face imaging methods developed here should facilitate understanding the function of apical structures in adult NSCs.

EXPERIMENTAL PROCEDURES

Animals and Stereotactic Injections

CD1 mice 2 to 4 months old (Charles River) and Aldh1L-GFP mice 2 months old were used to study the ventricular surface; 2- to 4-month old Z/EG mice (Novak et al., 2000) were used for adult LV injections; neonatal Z/EG mice used for radial glial targeting were sacrificed at 2–4 months. Striatal targeting of radial glia at P0 was performed as previously described (Merkle et al., 2004). Adult LV injections of 100 nl (in vivo experiments) or 500 nl (in vitro experiments) of adeno-GFAPp:Cre (Ad5 backbone, 1×10^{12} particles/ml) were performed at stereotactic coordinates (0 AP, 0.9 L, 1.9 D). All animal procedures were approved by the Institutional Animal Care and Use Committee.

Whole-Mount Dissection

After cervical dislocation, the brain was extracted fresh in L-15 at 37°C. The LV was dissected from the caudal aspect of the telencephalon, and the hippocampus and septum were removed. The dissected lateral wall was fixed in 4% PFA/0.1% TX overnight at 4°C. After staining, the ventricular walls were further dissected from underlying parenchyma as slivers of tissue 200–300 μm in thickness and mounted on a slide with mounting media and a coverslip.

Immunostaining and Microscopy

Primary and secondary antibodies were incubated in PBS with 0.5% TX and 10% normal goat or donkey serum for 24 hr at 4°C. For immunostaining of structures deeper within the SVZ, antibodies were incubated in PBS with

2% TX and 10% normal goat or donkey serum for 48 hr at 4°C. Primary antibodies were the following: mouse anti-acetylated tubulin (1:1000, Sigma T6793), rabbit anti-γ-tubulin (1:1000, Sigma T5192), mouse anti-γ-tubulin (1:500, Abcam ab11316), goat anti-γ-tubulin (1:200, Santa Cruz sc-7396), mouse anti-β-catenin (1:500, BD Transduction Labs 610153), rabbit anti-β-catenin (1:1000, Sigma C2206), rabbit anti-ZO1 (1:100, Zymed 40-2200), mouse anti-GFAP (1:500, Chemicon MAB3402), mouse IgM anti-vimentin (1:1000, Sigma V-2258), rabbit anti-S100β (1:500, DAKO A5110), mouse anti-nestin (1:200, Chemicon MAB353), rat anti-CD24 (1:500, BD PharMingen 557436), rat anti-CD133 (1:100, eBioscience 14-1331), chicken anti-GFP (1:500, Aves Labs GFP-1020), rabbit anti-phosphorylated histone H3 (1:500, Upstate 06-570), rabbit anti-doublecortin (1:500, Cell Signaling 4604), and rabbit anti-Ki67 (1:500, Vector VP-K451). Secondary antibodies were the following: conjugated to Alexa Fluor dyes (goat or donkey polyclonal, 1:400, Molecular Probes) and biotin (goat polyclonal, 1:250, Jackson ImmunoResearch) followed by streptavidin-HRP and diaminobenzidine. Confocal images were taken on a Nikon C1si or Leica SP5.

TEM analysis was performed as described (Doetsch et al., 1997). For reconstruction of type B1 and E2 cells, we cut ~600 serial ultrathin (0.05 μm) sections that were placed on Formvar-coated single-slot grids, stained with lead citrate, and examined under a Jeol 100CX EM.

Quantification of Cell Types

B1, E1, and E2 cells were counted in four nonoverlapping high-power fields (127 × 127 μm^2) from each of four regions (Figure S13). The number of each cell type was divided by the surface area to determine cell density. Data for all four regions were combined to determine average density across the entire whole mount.

Adherent NSC Cultures

Two days after unilateral injection of 500 nl adeno-GFAPp:Cre into the LV of Z/EG mice, the walls of the contralateral and ipsilateral LVs were dissected separately, dissociated, and used to establish adherent NSC cultures as previously described (Scheffler et al., 2005). After two passages under proliferation conditions, the NSC monolayers were allowed to differentiate for 7 days and fixed.

SUPPLEMENTAL DATA

The Supplemental Data include 13 figures and can be found with this article online at http://www.cellstemcell.com/cgi/content/full/3/3/265/DC1/.

ACKNOWLEDGMENTS

Work supported by National Institutes of Health (NIH) grant HD-32116, the Sandler Family Supporting Foundation, and the John G. Bowes Research Fund. Z.M. is supported by the Carlos Baldoceda Foundation and UCSF Krevans Fellowship. A.A.-B. holds the Heather and Melanie Muss Endowed Chair. We thank B. Barres for Aldh1L-GFP mice and Y.-G. Han, S. Noctor, R. Ihrie, J. Reiter, W. Marshall, and A. Javaherian for discussion. We thank K. Thorn and the UCSF Nikon Imaging Center for confocal imaging help. We thank Kenneth Xavier Probst for preparing the illustration in Figure 8.

Received: February 22, 2008
Revised: June 4, 2008
Accepted: July 7, 2008
Published: September 10, 2008

REFERENCES

Alvarez-Buylla, A., and Lim, D.A. (2004). For the long run: maintaining germinal niches in the adult brain. Neuron *41*, 683–686.

Alvarez-Buylla, A., and Nottebohm, F. (1988). Migration of young neurons in adult avian brain. Nature *335*, 353–354.

Alvarez-Buylla, A., Theelen, M., and Nottebohm, F. (1990). Proliferation "hot spots" in adult avian ventricular zone reveal radial cell division. Neuron *5*, 101–109.

Bittman, K., Owens, D.F., Kriegstein, A.R., and LoTurco, J.J. (1997). Cell coupling and uncoupling in the ventricular zone of developing neocortex. J. Neurosci. *17*, 7037–7044.

Breunig, J.J., Silbereis, J., Vaccarino, F.M., Sestan, N., and Rakic, P. (2007). Notch regulates cell fate and dendrite morphology of newborn neurons in the postnatal dentate gyrus. Proc. Natl. Acad. Sci. USA *104*, 20558–20563.

Bruni, J.E., Del Bigio, M.R., and Clattenburg, R.E. (1985). Ependyma: normal and pathological. A review of the literature. Brain Res. Brain Res. Rev. *9*, 1–19.

Cahoy, J.D., Emery, B., Kaushal, A., Foo, L.C., Zamanian, J.L., Christopherson, K.S., Xing, Y., Lubischer, J.L., Krieg, P.A., Krupenko, S.A., et al. (2008). A transcriptome database for astrocytes, neurons, and oligodendrocytes: a new resource for understanding brain development and function. J. Neurosci. *28*, 264–278.

Calaora, V., Chazal, G., Nielsen, P.J., Rougon, G., and Moreau, H. (1996). mCD24 expression in the developing mouse brain and in zones of secondary neurogenesis in the adult. Neuroscience *73*, 581–594.

Chenn, A., and Walsh, C.A. (2002). Regulation of cerebral cortical size by control of cell cycle exit in neural precursors. Science *297*, 365–369.

Cho, S.R., Benraiss, A., Chmielnicki, E., Samdani, A., Economides, A., and Goldman, S.A. (2007). Induction of neostriatal neurogenesis slows disease progression in a transgenic murine model of Huntington disease. J. Clin. Invest. *117*, 2889–2902.

Cohen, E., Binet, S., and Meininger, V. (1988). Ciliogenesis and centriole formation in the mouse embryonic nervous system. An ultrastructural analysis. Biol. Cell *62*, 165–169.

Committee, T.B. (1970). Embryonic vertebrate central nervous system: revised terminology. Anat. Rec. *166*, 257–262.

Corbit, K.C., Aanstad, P., Singla, V., Norman, A.R., Stainier, D.Y., and Reiter, J.F. (2005). Vertebrate Smoothened functions at the primary cilium. Nature *437*, 1018–1021.

Coskun, V., Wu, H., Blanchi, B., Tsao, S., Kim, K., Zhao, J., Biancotti, J.C., Hutnick, L., Krueger, R.C., Jr., Fan, G., et al. (2008). CD133+ neural stem cells in the ependyma of mammalian postnatal forebrain. Proc. Natl. Acad. Sci. USA *105*, 1026–1031.

Del Brio, M.A., Riera, P., García, J.M., and Alvarez-Uría, M. (1991). Cell types of the third ventricle wall of the rabbit (*Oryctolagus cuniculus*). J. Submicrosc. Cytol. Pathol. *23*, 147–157.

Del Carmen Gomez-Roldan, M., Perez-Martin, M., Capilla-Gonzalez, V., Cifuentes, M., Perez, J., Garcia-Verdugo, J.M., and Fernandez-Llebrez, P. (2008). Neuroblast proliferation on the surface of the adult rat striatal wall after focal ependymal loss by intracerebroventricular injection of neuraminidase. J. Comp. Neurol. *507*, 1571–1587.

Doetsch, F., and Alvarez-Buylla, A. (1996). Network of tangential pathways for neuronal migration in adult mammalian brain. Proc. Natl. Acad. Sci. USA *93*, 14895–14900.

Doetsch, F., Garcia-Verdugo, J.M., and Alvarez-Buylla, A. (1997). Cellular composition and three-dimensional organization of the subventricular germinal zone in the adult mammalian brain. J. Neurosci. *17*, 5046–5061.

Doetsch, F., Caille, I., Lim, D.A., García-Verdugo, J.M., and Alvarez-Buylla, A. (1999a). Subventricular zone astrocytes are neural stem cells in the adult mammalian brain. Cell *97*, 1–20.

Doetsch, F., Garcia-Verdugo, J.M., and Alvarez-Buylla, A. (1999b). Regeneration of a germinal layer in the adult mammalian brain. Proc. Natl. Acad. Sci. USA *96*, 11619–11624.

Dubreuil, V., Marzesco, A.M., Corbeil, D., Huttner, W.B., and Wilsch-Brauninger, M. (2007). Midbody and primary cilium of neural progenitors release extracellular membrane particles enriched in the stem cell marker prominin-1. J. Cell Biol. *176*, 483–495.

Flament-Durand, J., and Brion, J.P. (1985). Tanycytes: morphology and functions. A review. Int. Rev. Cytol. *96*, 121–155.

Garcia, A.D., Doan, N.B., Imura, T., Bush, T.G., and Sofroniew, M.V. (2004). GFAP-expressing progenitors are the principal source of constitutive neurogenesis in adult mouse forebrain. Nat. Neurosci. *7*, 1233–1241.

Garcia-Verdugo, J.M., Ferron, S., Flames, N., Collado, L., Desfilis, E., and Font, E. (2002). The proliferative ventricular zone in adult vertebrates: a comparative study using reptiles, birds, and mammals. Brain Res. Bull. *57*, 765–775.

Gerdes, J.M., Liu, Y., Zaghloul, N.A., Leitch, C.C., Lawson, S.S., Kato, M., Beachy, P.A., Beales, P.L., Demartino, G.N., Fisher, S., et al. (2007). Disruption of the basal body compromises proteasomal function and perturbs intracellular Wnt response. Nat. Genet. *39*, 1350–1360.

Goldman, S.A., Zukhar, A., Barami, K., Mikawa, T., and Niedzwiecki, D. (1996). Ependymal/subependymal zone cells of postnatal and adult songbird brain generate both neurons and nonneuronal siblings *in vitro* and *in vivo*. J. Neurobiol. *30*, 505–520.

Halfter, W., Dong, S., Yip, Y.P., Willem, M., and Mayer, U. (2002). A critical function of the pial basement membrane in cortical histogenesis. J. Neurosci. *22*, 6029–6040.

Haubst, N., Georges-Labouesse, E., De Arcangelis, A., Mayer, U., and Gotz, M. (2006). Basement membrane attachment is dispensable for radial glial cell fate and for proliferation, but affects positioning of neuronal subtypes. Development *133*, 3245–3254.

Huangfu, D., Liu, A., Rakeman, A.S., Murcia, N.S., Niswander, L., and Anderson, K.V. (2003). Hedgehog signalling in the mouse requires intraflagellar transport proteins. Nature *426*, 83–87.

Jackson, E.L., and Alvarez-Buylla, A. (2008). Characterization of adult neural stem cells and their relation to brain tumors. Cells Tissues Organs *188*, 212–224.

Jackson, E.L., Garcia-Verdugo, J.M., Gil-Perotin, S., Roy, M., Quinones-Hinojosa, A., Vandenberg, S., and Alvarez-Buylla, A. (2006). PDGFRalpha-positive B cells are neural stem cells in the adult SVZ that form glioma-like growths in response to increased PDGF signaling. Neuron *51*, 187–199.

Jiang, J., McMurtry, J., Niedzwiecki, D., and Goldman, S.A. (1998). Insulin-like growth factor-1 is a radial cell-associated neurotrophin that promotes neuronal recruitment from the adult songbird ependyma/subependyma. J. Neurobiol. *36*, 1–15.

Kerever, A., Schnack, J., Vellinga, D., Ichikawa, N., Moon, C., Arikawa-Hirasawa, E., Efird, J.T., and Mercier, F. (2007). Novel extracellular matrix structures in the neural stem cell niche capture the neurogenic factor fibroblast growth factor 2 from the extracellular milieu. Stem Cells *25*, 2146–2157.

Kosodo, Y., Roper, K., Haubensak, W., Marzesco, A.M., Corbeil, D., and Huttner, W.B. (2004). Asymmetric distribution of the apical plasma membrane during neurogenic divisions of mammalian neuroepithelial cells. EMBO J. *23*, 2314–2324.

Kuo, C.T., Mirzadeh, Z., Soriano-Navarro, M., Rasin, M., Wang, D., Shen, J., Sestan, N., Garcia-Verdugo, J., Alvarez-Buylla, A., Jan, L.Y., et al. (2006). Postnatal deletion of Numb/Numblike reveals repair and remodeling capacity in the subventricular neurogenic niche. Cell *127*, 1253–1264.

Leventhal, C., Rafii, S., Rafii, D., Shahar, A., and Goldman, S. (1999). Endothelial trophic support of neuronal production and recruitment from the adult mammalian subependyma. Mol. Cell. Neurosci. *13*, 450–464.

Lim, D.A., Tramontin, A.D., Trevejo, J.M., Herrera, D.G., Garcia-Verdugo, J.M., and Alvarez-Buylla, A. (2000). Noggin antagonizes BMP signaling to create a niche for adult neurogenesis. Neuron *28*, 713–726.

Lois, C., Garcia-Verdugo, J.M., and Alvarez-Buylla, A. (1996). Chain migration of neuronal precursors. Science *271*, 978–981.

Luo, J., Shook, B.A., Daniels, S.B., and Conover, J.C. (2008). Subventricular zone-mediated ependyma repair in the adult mammalian brain. J. Neurosci. *28*, 3804–3813.

Manabe, N., Hirai, S., Imai, F., Nakanishi, H., Takai, Y., and Ohno, S. (2002). Association of ASIP/mPAR-3 with adherens junctions of mouse neuroepithelial cells. Dev. Dyn. *225*, 61–69.

Mercier, F., Kitasako, J.T., and Hatton, G.I. (2002). Anatomy of the brain neurogenic zones revisited: fractones and the fibroblast/macrophage network. J. Comp. Neurol. *451*, 170–188.

Merkle, F.T., Tramontin, A.D., Garcia-Verdugo, J.M., and Alvarez-Buylla, A. (2004). Radial glia give rise to adult neural stem cells in the subventricular zone. Proc. Natl. Acad. Sci. USA *101*, 17528–17532.

Merkle, F.T., Mirzadeh, Z., and Alvarez-Buylla, A. (2007). Mosaic organization of neural stem cells in the adult brain. Science *317*, 381–384.

Misson, J.P., Edwards, M.A., Yamamoto, M., and Caviness, V.S., Jr. (1988). Mitotic cycling of radial glial cells of the fetal murine cerebral wall: a combined autoradiographic and immunohistochemical study. Brain Res. Dev. Brain Res. *38*, 183–190.

Nadarajah, B., Jones, A.M., Evans, W.H., and Parnavelas, J.G. (1997). Differential expression of connexins during neocortical development and neuronal circuit formation. J. Neurosci. *17*, 3096–3111.

Noctor, S.C., Flint, A.C., Weissman, T.A., Dammerman, R.S., and Kriegstein, A.R. (2001). Neurons derived from radial glial cells establish radial units in neocortex. Nature *409*, 714–720.

Noctor, S.C., Martinez-Cerdeno, V., and Kriegstein, A.R. (2007a). Contribution of intermediate progenitor cells to cortical histogenesis. Arch. Neurol. *64*, 639–642.

Noctor, S.C., Martinez-Cerdeno, V., and Kriegstein, A.R. (2007b). Neural stem and progenitor cells in cortical development. Novartis Found. Symp. *288*, 59–78.

Novak, A., Guo, C., Yang, W., Nagy, A., and Lobe, C.G. (2000). Z/EG, a double reporter mouse line that expresses enhanced green fluorescent protein upon Cre-mediated excision. Genesis *28*, 147–155.

Ou, Y., Zhang, M., and Rattner, J.B. (2004). The centrosome: The centriole-PCM coalition. Cell Motil. Cytoskeleton *57*, 1–7.

Palmer, T.D., Willhoite, A.R., and Gage, F.H. (2000). Vascular niche for adult hippocampal neurogenesis. J. Comp. Neurol. *425*, 479–494.

Peretto, P., Merighi, A., Fasolo, A., and Bonfanti, L. (1997). Glial tubes in the rostral migratory stream of the adult rat. Brain Res. Bull. *42*, 9–21.

Peretto, P., Dati, C., De Marchis, S., Kim, H.H., Ukhanova, M., Fasolo, A., and Margolis, F.L. (2004). Expression of the secreted factors noggin and bone morphogenetic proteins in the subependymal layer and olfactory bulb of the adult mouse brain. Neuroscience *128*, 685–696.

Pincus, D.W., Keyoung, H.M., Harrison-Restelli, C., Goodman, R.R., Fraser, R.A.R., Edgar, M., Sakakibara, S., Okano, H., Nedergaard, M., and Goldman, S.A. (1998). Fibroblast growth factor-2/brain-derived neurotrophic factor-associated maturation of new neurons generated from adult human subependymal cells. Ann. Neurol. *43*, 576–585.

Rakic, P. (1972). Mode of cell migration to the superficial layers of fetal monkey neocortex. J. Comp. Neurol. *145*, 61–84.

Rasin, M.R., Gazula, V.R., Breunig, J.J., Kwan, K.Y., Johnson, M.B., Liu-Chen, S., Li, H.S., Jan, L.Y., Jan, Y.N., Rakic, P., et al. (2007). Numb and Numbl are required for maintenance of cadherin-based adhesion and polarity of neural progenitors. Nat. Neurosci. *10*, 819–827.

Rohatgi, R., Milenkovic, L., and Scott, M.P. (2007). Patched1 regulates hedgehog signaling at the primary cilium. Science *317*, 372–376.

Sanai, N., Tramontin, A.D., Quinones-Hinojosa, A., Barbaro, N.M., Gupta, N., Kunwar, S., Lawton, M.T., McDermott, M.W., Parsa, A.T., Manuel-Garcia Verdugo, J., et al. (2004). Unique astrocyte ribbon in adult human brain contains neural stem cells but lacks chain migration. Nature *427*, 740–744.

Sawamoto, K., Wichterle, H., Gonzalez-Perez, O., Cholfin, J.A., Yamada, M., Spassky, N., Murcia, N.S., Garcia-Verdugo, J.M., Marin, O., Rubenstein, J.L., et al. (2006). New neurons follow the flow of cerebrospinal fluid in the adult brain. Science *311*, 629–632.

Scheffler, B., Walton, N.M., Lin, D.D., Goetz, A.K., Enikolopov, G., Roper, S.N., and Steindler, D.A. (2005). Phenotypic and functional characterization of adult brain neuropoiesis. Proc. Natl. Acad. Sci. USA *102*, 9353–9358.

Scholzen, T., and Gerdes, J. (2000). The Ki-67 protein: from the known and the unknown. J. Cell. Physiol. *182*, 311–322.

Shen, Q., Goderie, S.K., Jin, L., Karanth, N., Sun, Y., Abramova, N., Vincent, P., Pumiglia, K., and Temple, S. (2004). Endothelial cells stimulate self-renewal and expand neurogenesis of neural stem cells. Science *304*, 1338–1340.

Shingo, T., Gregg, C., Enwere, E., Fujikawa, H., Hassam, R., Geary, C., Cross, J.C., and Weiss, S. (2003). Pregnancy-stimulated neurogenesis in the adult female forebrain mediated by prolactin. Science *299*, 117–120.

Sorokin, S.P. (1968). Reconstructions of centriole formation and ciliogenesis in mammalian lungs. J. Cell Sci. *3*, 207–230.

Spassky, N., Merkle, F.T., Flames, N., Tramontin, A.D., Garcia-Verdugo, J.M., and Alvarez-Buylla, A. (2005). Adult ependymal cells are postmitotic and are derived from radial glial cells during embryogenesis. J. Neurosci. *25*, 10–18.

Uchida, N., Buck, D.W., He, D., Reitsma, M.J., and Masek, M. (2000). Direct isolation of human central nervous system stem cells. Proc. Natl. Acad. Sci. USA *97*, 14720–14725.

Voigt, T. (1989). Development of glial cells in the cerebral wall of ferrets: direct tracing of their transformation from radial glia into astrocytes. J. Comp. Neurol. *289*, 74–88.

Weigmann, A., Corbeil, D., Hellwig, A., and Huttner, W.B. (1997). Prominin, a novel microvilli-specific polytopic membrane protein of the apical surface of epithelial cells, is targeted to plasmalemmal protrusions of non-epithelial cells. Proc. Natl. Acad. Sci. USA *94*, 12425–12430.

Weissman, T.A., Riquelme, P.A., Ivic, L., Flint, A.C., and Kriegstein, A.R. (2004). Calcium waves propagate through radial glial cells and modulate proliferation in the developing neocortex. Neuron *43*, 647–661.

Zhao, C., Deng, W., and Gage, F.H. (2008). Mechanisms and functional implications of adult neurogenesis. Cell *132*, 645–660.